

TTP07-32
 SFB/CPP-07-76
 arXiv:0711.2636

Higher Moments of Heavy Quark Correlators in the Low Energy Limit at $\mathcal{O}(\alpha_s^2)$

A. Maier^a, P. Maierhöfer^a and P. Marquard^a

^a*Institut für Theoretische Teilchenphysik, Universität Karlsruhe, 76128 Karlsruhe,
 Germany*

Abstract

We present the first 30 moments of the low energy expansions of the vector, axial-vector, scalar and pseudo-scalar heavy quark correlation functions at three-loop order, including the singlet contribution which appears for the first time at three loops. In addition we compare the behavior of the moments for large n with the prediction from threshold calculations.

Key words: Heavy quarks

1 Introduction

Correlators of two currents $j_{[\mu]}(x)$, where $j_{[\mu]}(x)$ is the scalar $\bar{\psi}\psi$, pseudo-scalar $i\bar{\psi}\gamma_5\psi$, vector $\bar{\psi}\gamma_\mu\psi$, or axial-vector $\bar{\psi}\gamma_\mu\gamma_5\psi$ current, are important for many interesting phenomenological purposes. Their low energy expansions, in particular, are of interest for applications based on sum rules [1,2] like the determination of the charm and bottom quark mass from $R(s)$ [3,4].

In three-loop approximation, i. e. $\mathcal{O}(\alpha_s^2)$, the moments of the Taylor expansion for the four correlators were evaluated up to $(q^2)^8$ in [5] using recursion algorithms originally suggested in [6]. The series was evaluated in four-loop approximation up to the first physical moment $(q^2)^1$ [7,8] employing the Laporta algorithm [9]. The three-loop singlet contributions have been calculated in [10] up to the seventh and eighth moments for the axial-vector and the scalar and pseudo-scalar correlators, respectively.

Recently, using a completely different technique based on master differential

equations [11,12], the three-loop vector correlator has been calculated up to $(q^2)^{30}$ [13].

Higher moments of the pseudo-scalar correlator might be used to determine the impact of non-perturbative effects in the determination of quark masses from lattice calculations [14].

In this work we calculate the low energy expansions for the four types of correlators in order α_s^2 up to $(q^2)^{30}$, including the logarithms which arise from the singlet contribution, given by double triangle diagrams.

This paper is organized as follows: In Section 2 we briefly present the methods used in the calculation, paying special attention to the singlet parts. The results are presented in Section 3 where we also compare the explicitly calculated moments with the behavior for large powers of q^2 derived from the threshold region. Section 4 contains a brief summary and conclusions.

2 Definitions and Methods

The polarization functions are defined by

$$(-q^2 g_{\mu\nu} + q_\mu q_\nu) \Pi^\delta(q^2) + q_\mu q_\nu \Pi_L^\delta(q^2) = i \int dx e^{iqx} \langle 0 | T j_\mu^\delta(x) j_\nu^\delta(0) | 0 \rangle \quad (1)$$

for $\delta = v, a,$

$$q^2 \Pi^\delta(q^2) = i \int dx e^{iqx} \langle 0 | T j^\delta(x) j^\delta(0) | 0 \rangle \quad (2)$$

for $\delta = s, p,$

with the currents

$$j_\mu^v = \bar{\psi} \gamma_\mu \psi, \quad j_\mu^a = \bar{\psi} \gamma_\mu \gamma_5 \psi, \quad j^s = \bar{\psi} \psi, \quad j^p = i \bar{\psi} \gamma_5 \psi. \quad (3)$$

In the low energy limit the polarization functions can be written as a series in $z = \frac{q^2}{4m^2}$, where m is the mass of the heavy quark,

$$\Pi^\delta(q^2) = \frac{3}{16\pi^2} \sum_{n>0} C_n^\delta z^n, \quad (4)$$

with

$$C_n^\delta = C_n^{(0),\delta} + \frac{\alpha_s}{\pi} C_F C_n^{(1),\delta} + \left(\frac{\alpha_s}{\pi}\right)^2 C_n^{(2),\delta} + \dots , \quad (5)$$

$$\begin{aligned} C_n^{(2),\delta} &= C_F^2 C_{A,n}^{(2),\delta} + C_F C_A C_{NA,n}^{(2),\delta} + C_F T_F n_l C_{l,n}^{(2),\delta} \\ &\quad + C_F T_F n_h C_{F,n}^{(2),\delta} + C_F T_F n_h C_{S,n}^{(2),\delta}. \end{aligned} \quad (6)$$

The singlet contributions $C_{S,n}^{(2),\delta}$ arise from the diagrams shown in Fig. 2. It has to be noted that these are not simple power series in z but contain logarithms of the form $\log(-\frac{q^2}{m^2})$. This logarithmic dependence on q^2 reflects the presence of massless cuts in the diagrams.

The expansion in the limit $q^2 \rightarrow 0$ can be achieved in two different ways. One possibility is to first expand the propagators and later reduce the resulting massive tadpoles to master integrals. For each order in the z -expansion two more powers of the propagators arise. For large n this makes the reduction to master integrals through the reduction formalisms of Broadhurst or Laporta very cumbersome. The second possibility is the reduction of the full propagators to master integrals. These master integrals have then to be known at least as an expansion in the external momentum which can be calculated efficiently to high orders. The price to pay is the increased difficulty in obtaining the necessary reduction to master integrals. In this paper we choose the latter approach, which we present in more detail in the following.

In the first step, the diagrams are generated with **QGRAF** [15]. The occurring topologies are identified with the help of **q2e** and **exp** [16,17]. The integrals are reduced to scalar propagator-type integrals of the form

$$P(q^2, a_1, \dots, a_9) = \int \frac{[dk_1][dk_2][dk_3]}{D_1^{a_1} D_2^{a_2} \dots D_9^{a_9}} . \quad (7)$$

using the computer algebra program **FORM** [18]. The denominators are given by $D_i = (l - m_i^2 + i\varepsilon)$, where l is a linear combination of the loop momenta k_i and the external momentum q , and $m_i \in \{0, m\}$ is the mass of the corresponding propagator. Only one non-zero mass is taken into account for the heaviest quark, lighter quarks are treated as massless. The powers a_i of the denominators are integers. Irreducible scalar products are expressed as propagators with negative powers. The integrals are dimensionally regularized in space-time dimension $d = 4 - 2\epsilon$.

In a next step, Integration-by-Parts [19] and Laporta's algorithm [9,20] are used to reduce all needed integrals of the form (7) to master integrals. This reduction is done with the program **Crusher** [21]. **Crusher** uses **GiNaC** [22] for algebraic manipulations and **Fermat** [23] for the simplification of the intermediate expressions using a special interface [24]. As a result of the reduction one finds a total of 55 master integrals.

The master integrals have to be expanded for small external momenta around $q^2 = 0$. To achieve this, we use the scaling equation

$$\left(q^2 \frac{\partial}{\partial q^2} + m^2 \frac{\partial}{\partial m^2} - \hat{D} \right) M_i(q^2) = 0 \quad (8)$$

for the master integrals M_i . \hat{D} applied to M_i gives the mass dimension of M_i . Carrying out the mass derivative produces integrals with additional powers of propagators, that are again mapped to master integrals. This gives a system of coupled inhomogeneous linear differential equations in q^2 . For the non-singlet part, the system is solved by a Taylor series

$$M_i(q^2) = \sum_{k=0}^{\infty} M_i^{(k)}(q^2)^k , \quad (9)$$

where the coefficients $M_i^{(k)}$ have to be calculated. Diagrammatically, the coefficients are tadpole diagrams. As boundary conditions, the three-loop master tadpoles depicted in Fig. 1 (a)-(c) are chosen. The $M_i^{(k)}$ can be expressed as linear combinations of these. For the singlet part, non-integer powers of q^2 have to be taken into account:

$$M_i(q^2) = \sum_k \left(M_i^{(k)} + M_{i,s}^{(k)}(q^2)^{-\epsilon} + M_{i,ss}^{(k)}(q^2)^{-2\epsilon} \right) (q^2)^k . \quad (10)$$

In this case, the boundary conditions for the coefficients $M_{i,s}^{(k)}$ and $M_{i,ss}^{(k)}$ are the diagrams depicted in Fig. 1 (d) and (e), (f), respectively. Generation and solution of the system are implemented in a **Mathematica** program. With our setup we can calculate the q^2 expansion to almost arbitrary depths. In this work we limit ourselves to the first 30 moments. This way of calculating expansions of integrals was proposed in [11,12] and applied to the vector current in [13].

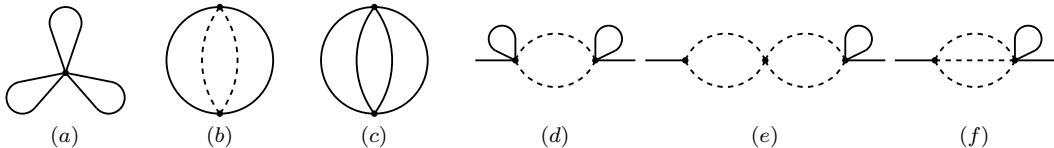


Fig. 1. Diagrams, which are chosen as boundary conditions for the expansion of the propagator-type master integrals in q^2 . The diagrams (d) – (f) contribute only to the singlet part.

To perform the renormalization we need the strong coupling α_s [25] and the mass renormalization constant at two-loop order [26,27,28].

For the pseudo-scalar and axial-vector currents we have to pay special attention to the treatment of γ_5 . While in the non-singlet contributions γ_5 can

simply be considered as anticommutating this is not possible for the singlet contributions. In the latter case the γ_5 matrix cannot easily be removed from the problem and has to be treated properly to avoid problems with dimensional regularization. Therefore we follow the prescription proposed by Larin [29] and use the definition $\gamma_5 = \frac{i}{4!} \epsilon_{\mu\nu\rho\sigma} \gamma^\mu \gamma^\nu \gamma^\rho \gamma^\sigma$. Since the ϵ -tensor is intrinsically a four-dimensional object it can not be used in dimensional regularization and has to be taken out of the calculation until the renormalization has been performed. Taking the ϵ -tensors out of the calculation the tensor structure of the pseudo-scalar and axial-vector correlators can be cast into the form

$$\Pi_{\mu'\nu'\rho'\sigma'}^{p\mu\nu\rho\sigma} = \Pi_1^p g_{[\mu'}^{[\mu} g_{\nu'}^{\nu} g_{\rho'}^{\rho} g_{\sigma']}^{\sigma]} + \Pi_2^p q^{[\mu} q_{[\mu'} g_{\nu'}^{\nu} g_{\rho'}^{\rho} g_{\sigma']}^{\sigma]} , \quad (11)$$

$$\Pi_{\mu'\nu'\rho'}^{a\mu\nu\rho} = \Pi_1^a g_{[\mu'}^{[\mu} g_{\nu'}^{\nu} g_{\rho']}^{\rho]} + \Pi_2^a q^{[\mu} q_{[\mu'} g_{\nu'}^{\nu} g_{\rho']}^{\rho]} , \quad (12)$$

where $[...]$ denotes total antisymmetrization. After renormalization these expressions can be multiplied with the ϵ -tensors to obtain the final result. The correlators are then given by

$$\Pi^p = \Pi_1^p + \Pi_2^p , \quad (13)$$

$$\Pi^a = \Pi_1^a + \Pi_2^a , \quad (14)$$

$$\Pi_L^a = \Pi_2^a . \quad (15)$$

The pseudo-scalar and the longitudinal part of the axial-vector correlator are connected through a Ward identity.

$$q^2 \Pi_L^a(q^2) = 4m^2 (\Pi^p(q^2) - q^2 (\partial \Pi^p(q^2) / \partial q^2)|_{q^2=0}) . \quad (16)$$

In order to retain this Ward identity for the singlet contribution it is necessary to cancel the axial-vector anomaly. For this reason we computed the singlet part $\Pi_{\mu\nu,S}$ of the axial-vector correlator for an isospin doublet (ψ, χ) , where ψ is taken to be heavy and χ light. The diagrams contributing to the full singlet part are depicted in Fig. 2. Note that the completely massless diagram does only contribute to the leading moment.

3 Results and asymptotic behavior for large n

The numerical results¹ for the first 30 moments of the various currents are listed in Appendix A. The results are given in both the $\overline{\text{MS}}$ and the onshell scheme since both schemes have their own range of applications. For convenience we set the renormalization scale $\mu = m$. Since the longitudinal part of

¹ While we agree in general with the results given in [13], we disagree with several single digits.

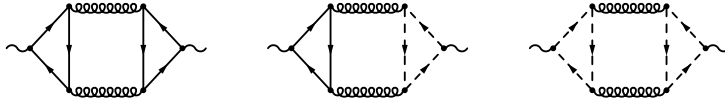


Fig. 2. Diagrams for the singlet contribution. The first diagram contributes to scalar, pseudo-scalar and axial-vector correlators, while the latter two are only taken into account for the axial-vector to cancel the anomaly. Solid and dashed lines denote massive and massless lines, respectively.

the axial-vector correlator can be easily obtained from the pseudo-scalar one by use of the Ward identity (16) we give only the results for the transversal part in this case.

The results for the singlet contributions to the scalar, pseudo-scalar and axial-vector correlators can be split into a constant and a logarithmic part proportional to $\log(-\frac{q^2}{m^2})$. These are denoted by $C_{S,n}^{(2),\delta}[1]$ and $C_{S,n}^{(2),\delta}[L]$, respectively. In the case of the axial-vector correlator the singlet part includes contributions from heavy-light diagrams as explained in the previous section.

The corresponding analytical expressions for moments 9-12 in the $\overline{\text{MS}}$ scheme can be found in the Appendix B. The analytical results for all calculated moments both in the $\overline{\text{MS}}$ and onshell scheme including all logarithms are available in computer readable form from

<http://www-ttp.particle.uni-karlsruhe.de/Progdata/ttp07/ttp07-32>.

For large expansion depths, the moments can be compared to the asymptotic behavior, which follows from the threshold behavior of heavy quark production from e^+e^- .

$$C_{k,n} = \frac{4}{9} \int_{4m^2}^{\infty} \frac{ds}{s} R_k(s) \left(\frac{4m^2}{s} \right)^n = \frac{4}{9} \int_0^1 d(\beta^2) R_k(\beta) (1 - \beta^2)^{n-1}, \quad (17)$$

where

$$k = A, NA, l, F \quad \text{and} \quad \beta = \sqrt{1 - \frac{4m^2}{s}}. \quad (18)$$

In view of the smooth behavior of the calculated moments, we expect good agreement for $n \sim 30$. Large n expansions can be found in ref. [30] and derived from [31,5,32] by using eq. (17). A power β^j of the velocity in the R -ratio $R_k(\beta)$ corresponds to a power $n^{-1-j/2}$ of the large n expansion.

$$\begin{aligned}
C_{A,n}^{(2),v} &= \frac{\pi^{9/2}}{6} n^{-1/2} - 4\pi^2 n^{-1} + \frac{\sqrt{\pi}}{144} \left(23\pi^4 + 8\pi^2(6H_{n+\frac{1}{2}} \right. \\
&\quad \left. - 47 + 36\log(2)) + 36(39 - 4\zeta_3) \right) n^{-3/2} + \mathcal{O}(n^{-2}), \\
C_{NA,n}^{(2),v} &= \frac{\pi^2}{36} \left(33H_n + 31 - 66\log(2) \right) n^{-1} + \frac{\sqrt{\pi}}{72} \left(\pi^2(36H_{n+\frac{1}{2}} \right. \\
&\quad \left. + 107 - 120\log(2)) - 302 - 468\zeta_3 \right) n^{-3/2} + \mathcal{O}(n^{-2}), \\
C_{l,n}^{(2),v} &= -\frac{\pi^2}{9} \left(3H_n + 5 - 6\log(2) \right) n^{-1} + \frac{11\sqrt{\pi}}{9} n^{-3/2} + \mathcal{O}(n^{-2}), \\
C_{F,n}^{(2),v} &= -\frac{4\sqrt{\pi}}{9} \left(\pi^2 - 11 \right) n^{-3/2} + \frac{\sqrt{\pi}}{54} \left(33\pi^2 - 344 \right) n^{-5/2} + \mathcal{O}(n^{-7/2}),
\end{aligned} \tag{19}$$

where H_n is the harmonic number given by

$$H_n = \sum_{i=1}^n \frac{1}{i} \tag{20}$$

for integer arguments or its generalization

$$H_n = \gamma_E + \psi_0(n+1) \tag{21}$$

for non-integer arguments, where γ_E is Euler's constant and ψ_0 is the digamma function. The asymptotic behavior is in both cases given by

$$H_n \approx \gamma_E + \log(n) + \mathcal{O}(n^{-1}) . \tag{22}$$

The comparison is shown for the vector current separately for each color factor in Fig. 3-6. The behavior of the leading order approximation is worst for the $C_{A,n}^{(2),v}$ contribution since the series starts with $\mathcal{O}(n^{-1/2})$ compared with at least $\mathcal{O}(n^{-1})$ for the other color factors. Comparing identical orders in the n expansion of the various color structures shows roughly the same degree of convergence, but the $C_{A,n}^{(2),v}$ is still penalized by the bad leading approximation. Overall we find good agreement between the large n expansion and the analytical moments. Also at two-loops this procedure shows nearly perfect agreement if one includes two terms in the large n expansion as can be seen in Fig. 7 .

4 Conclusion

We calculated the low-energy expansion of the heavy quark correlator for the scalar, pseudo-scalar, vector and axial-vector current up to $\left(\frac{q^2}{4m^2}\right)^{30}$ in three-loop approximation. For the scalar, pseudo-scalar and axial-vector currents

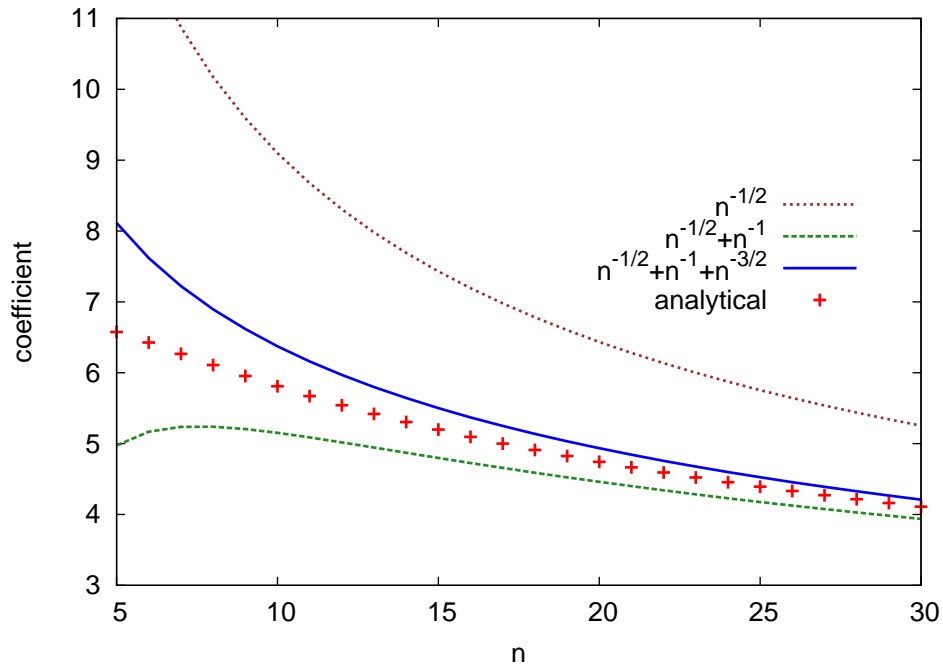


Fig. 3. Analytical moments compared to the large n expansion to different depths for the $C_{A,n}^{(2),v}$ part.

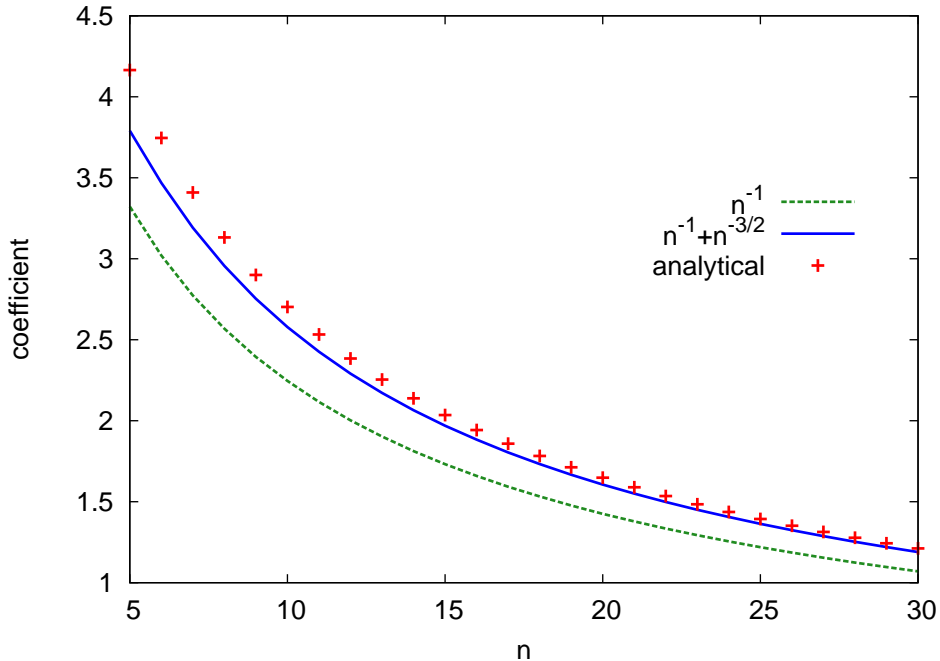


Fig. 4. Analytical moments compared to the large n expansion to different depths for the $C_{NA,n}^{(2),v}$ part.

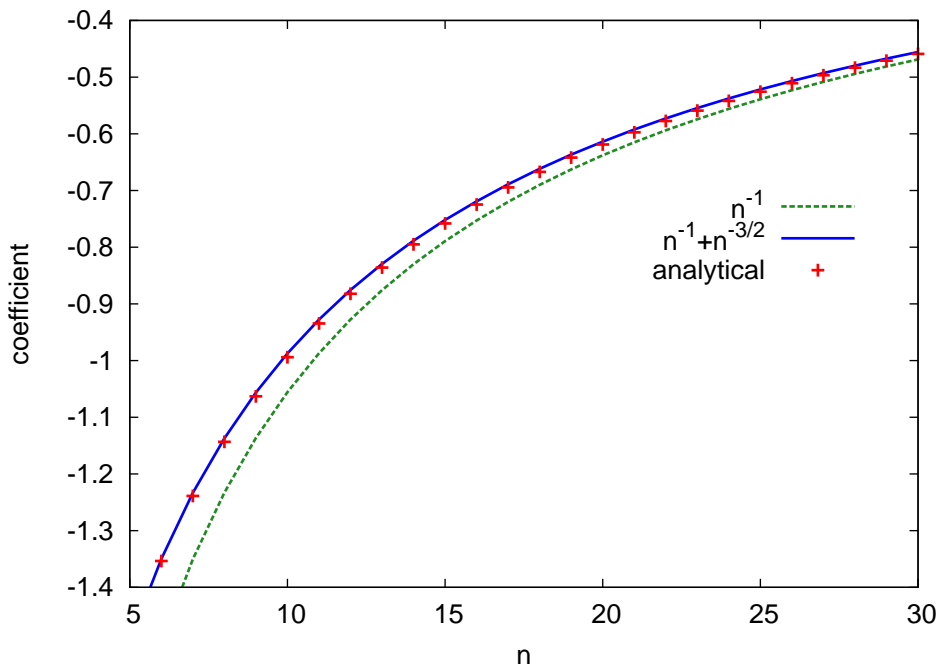


Fig. 5. Analytical moments compared to the large n expansion to different depths for the $C_{l,n}^{(2),v}$ part.

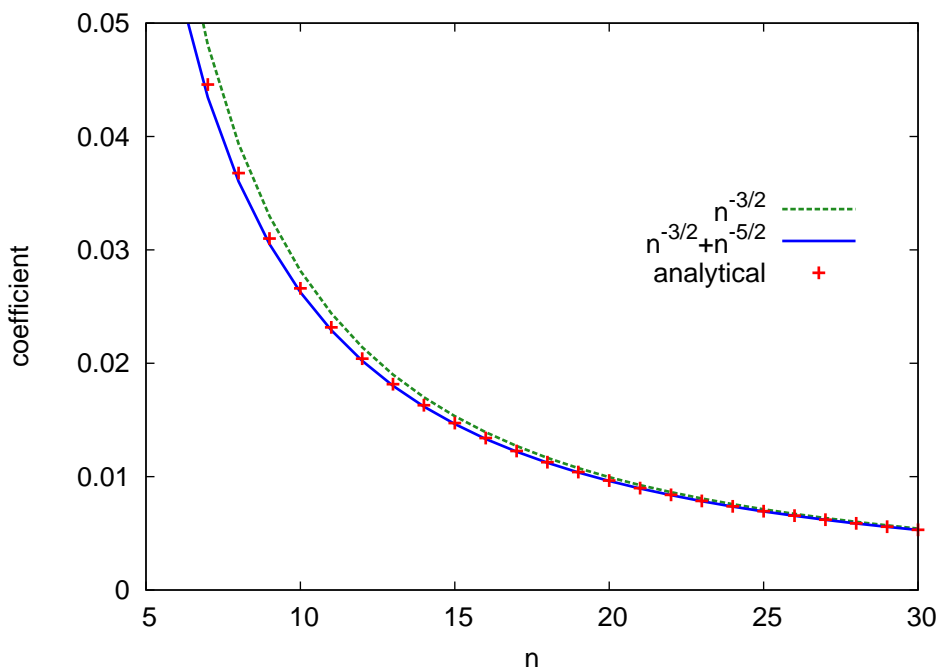


Fig. 6. Analytical moments compared to the large n expansion to different depths for the $C_{F,n}^{(2),v}$ part.

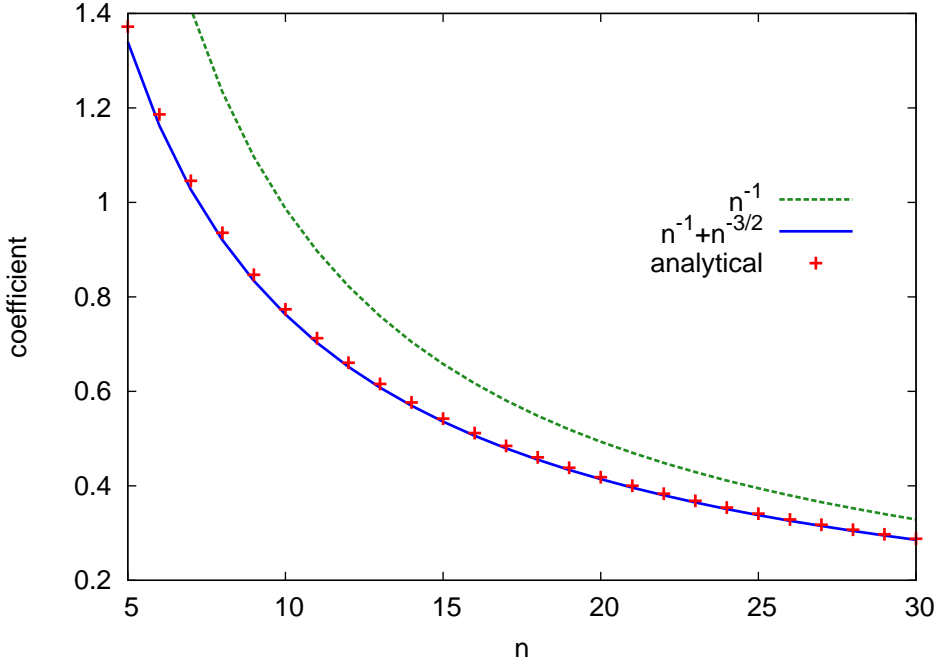


Fig. 7. Analytical moments compared to the large n expansion to different depths for the $C_n^{(1),v}$ part.

we included the singlet contributions arising from double triangle diagrams. Furthermore, for the vector current we compared the large n behavior of the moments with the asymptotic form derived from threshold behavior. Taking the lowest two or three terms of the $1/n$ expansion into account, we find good agreement between the asymptotic formulae and the explicit results.

Acknowledgments

We like to thank J. H. Kühn, K. Chetyrkin and M. Steinhauser for fruitful discussions. This work was supported by the DFG through SFB/TR 9. The work of Ph. M. was supported by the Graduiertenkolleg “Hochenergiephysik und Teilchenastrophysik”.

A Numerical results

n	$C_n^{(0),v}$	$C_n^{(1),v}$	$C_{A,n}^{(2),v}$	$C_{NA,n}^{(2),v}$	$C_{l,n}^{(2),v}$	$C_{F,n}^{(2),v}$
1	1.067	1.916	0.1541	-0.006971	0.9934	0.3956
2	0.4571	0.8322	0.3025	0.2215	0.6824	-0.01696
3	0.2709	0.3895	0.2711	-0.01532	0.6433	-0.1026
4	0.1847	0.1523	0.2785	-0.2218	0.6372	-0.1301
5	0.1364	0.007970	0.3424	-0.3775	0.6362	-0.1396
6	0.1061	-0.08688	0.4535	-0.4936	0.6351	-0.1421
7	0.08558	-0.1525	0.6007	-0.5813	0.6329	-0.1415
8	0.07094	-0.1995	0.7750	-0.6484	0.6297	-0.1396
9	0.06006	-0.2342	0.9694	-0.7004	0.6257	-0.1369
10	0.05170	-0.2602	1.179	-0.7412	0.6211	-0.1340
11	0.04512	-0.2801	1.400	-0.7734	0.6162	-0.1310
12	0.03983	-0.2954	1.629	-0.7991	0.6110	-0.1281
13	0.03550	-0.3073	1.864	-0.8195	0.6056	-0.1252
14	0.03190	-0.3166	2.104	-0.8359	0.6002	-0.1225
15	0.02887	-0.3239	2.347	-0.8490	0.5948	-0.1198
16	0.02629	-0.3296	2.592	-0.8595	0.5894	-0.1173
17	0.02408	-0.3339	2.838	-0.8677	0.5841	-0.1149
18	0.02216	-0.3373	3.085	-0.8742	0.5788	-0.1126
19	0.02048	-0.3398	3.333	-0.8793	0.5737	-0.1105
20	0.01900	-0.3417	3.581	-0.8830	0.5686	-0.1084
21	0.01770	-0.3430	3.828	-0.8858	0.5636	-0.1065
22	0.01653	-0.3438	4.074	-0.8877	0.5587	-0.1046
23	0.01549	-0.3443	4.319	-0.8888	0.5540	-0.1028
24	0.01455	-0.3444	4.564	-0.8894	0.5493	-0.1011
25	0.01371	-0.3443	4.807	-0.8894	0.5448	-0.09953
26	0.01294	-0.3439	5.049	-0.8889	0.5404	-0.09798
27	0.01224	-0.3434	5.290	-0.8881	0.5360	-0.09650
28	0.01161	-0.3427	5.529	-0.8870	0.5318	-0.09509
29	0.01102	-0.3419	5.767	-0.8855	0.5277	-0.09373
30	0.01049	-0.3410	6.003	-0.8839	0.5237	-0.09243

Table A.1
Moments for the vector correlator in the $\overline{\text{MS}}$ scheme

n	$C_n^{(0),v}$	$C_n^{(1),v}$	$C_{A,n}^{(2),v}$	$C_{NA,n}^{(2),v}$	$C_{l,n}^{(2),v}$	$C_{F,n}^{(2),v}$
1	1.067	4.049	5.075	7.098	-2.339	0.7270
2	0.4571	2.661	6.393	6.311	-2.174	0.2671
3	0.2709	2.015	6.689	5.398	-1.896	0.1499
4	0.1847	1.630	6.685	4.699	-1.671	0.09947
5	0.1364	1.372	6.574	4.165	-1.494	0.07230
6	0.1061	1.186	6.426	3.746	-1.353	0.05566
7	0.08558	1.046	6.267	3.409	-1.239	0.04459
8	0.07094	0.9356	6.108	3.132	-1.143	0.03677
9	0.06006	0.8469	5.955	2.900	-1.063	0.03100
10	0.05170	0.7738	5.809	2.702	-0.9941	0.02661
11	0.04512	0.7126	5.671	2.532	-0.9345	0.02317
12	0.03983	0.6605	5.542	2.384	-0.8822	0.02041
13	0.03550	0.6156	5.420	2.254	-0.8361	0.01816
14	0.03190	0.5765	5.305	2.139	-0.7950	0.01629
15	0.02887	0.5422	5.198	2.035	-0.7581	0.01473
16	0.02629	0.5118	5.096	1.943	-0.7248	0.01340
17	0.02408	0.4847	5.000	1.858	-0.6946	0.01226
18	0.02216	0.4603	4.910	1.782	-0.6671	0.01127
19	0.02048	0.4383	4.824	1.712	-0.6419	0.01041
20	0.01900	0.4184	4.743	1.648	-0.6187	0.009654
21	0.01770	0.4002	4.665	1.589	-0.5973	0.008984
22	0.01653	0.3836	4.592	1.535	-0.5775	0.008389
23	0.01549	0.3683	4.522	1.484	-0.5590	0.007857
24	0.01455	0.3541	4.455	1.437	-0.5419	0.007379
25	0.01371	0.3411	4.392	1.393	-0.5258	0.006947
26	0.01294	0.3290	4.331	1.352	-0.5108	0.006556
27	0.01224	0.3177	4.272	1.314	-0.4967	0.006201
28	0.01161	0.3072	4.216	1.277	-0.4834	0.005876
29	0.01102	0.2974	4.162	1.243	-0.4709	0.005579
30	0.01049	0.2881	4.111	1.211	-0.4590	0.005306

Table A.2

Moments for the vector correlator in the onshell scheme

n	$C_n^{(0),a}$	$C_n^{(1),a}$	$C_{A,n}^{(2),a}$	$C_{NA,n}^{(2),a}$	$C_{l,n}^{(2),a}$	$C_{F,n}^{(2),a}$	$C_{S,n}^{(2),a}[1]$	$C_{S,n}^{(2),a}[L]$
1	0.53330	0.6346	0.5003	-0.8386	0.6198	0.1775	1.970	-0.6914
2	0.15240	0.1062	0.3025	-0.3370	0.2883	-0.02960	0.3832	-0.1867
3	0.06772	-0.009570	0.2271	-0.2631	0.2034	-0.04074	0.1447	-0.08050
4	0.03694	-0.04310	0.2071	-0.2263	0.1602	-0.03578	0.07290	-0.04309
5	0.02273	-0.05255	0.2079	-0.1987	0.1323	-0.02992	0.04308	-0.02618
6	0.01516	-0.05367	0.2160	-0.1764	0.1124	-0.02505	0.02813	-0.01729
7	0.01070	-0.05172	0.2261	-0.1578	0.09739	-0.02121	0.01966	-0.01212
8	0.007883	-0.04869	0.2363	-0.1422	0.08563	-0.01820	0.01443	-0.008880
9	0.006006	-0.04540	0.2456	-0.1290	0.07617	-0.01580	0.01098	-0.006736
10	0.004700	-0.04219	0.2539	-0.1177	0.06841	-0.01388	0.008609	-0.005252
11	0.003760	-0.03919	0.2610	-0.1079	0.06193	-0.01230	0.006905	-0.004189
12	0.003064	-0.03644	0.2671	-0.09949	0.05646	-0.01099	0.005646	-0.003404
13	0.002536	-0.03394	0.2723	-0.09209	0.05177	-0.009902	0.004690	-0.002811
14	0.002127	-0.03168	0.2767	-0.08558	0.04772	-0.008976	0.003949	-0.002353
15	0.001804	-0.02963	0.2803	-0.07982	0.04420	-0.008185	0.003364	-0.001993
16	0.001547	-0.02779	0.2833	-0.07469	0.04109	-0.007502	0.002895	-0.001706
17	0.001338	-0.02612	0.2858	-0.07010	0.03835	-0.006909	0.002514	-0.001473
18	0.001166	-0.02460	0.2879	-0.06597	0.03591	-0.006389	0.002200	-0.001283
19	0.001024	-0.02322	0.2895	-0.06224	0.03373	-0.005931	0.001938	-0.001125
20	0.0009049	-0.02196	0.2909	-0.05886	0.03176	-0.005525	0.001719	-0.0009933
21	0.0008043	-0.02081	0.2919	-0.05578	0.02999	-0.005162	0.001533	-0.0008821
22	0.0007188	-0.01975	0.2926	-0.05296	0.02837	-0.004838	0.001375	-0.0007876
23	0.0006454	-0.01878	0.2932	-0.05039	0.02691	-0.004546	0.001238	-0.0007067
24	0.0005821	-0.01789	0.2935	-0.04802	0.02556	-0.004282	0.001120	-0.0006370
25	0.0005272	-0.01706	0.2937	-0.04583	0.02433	-0.004043	0.001017	-0.0005765
26	0.0004793	-0.01630	0.2937	-0.04381	0.02320	-0.003825	0.0009275	-0.0005238
27	0.0004372	-0.01559	0.2936	-0.04194	0.02216	-0.003626	0.0008484	-0.0004776
28	0.0004002	-0.01493	0.2934	-0.04020	0.02119	-0.003444	0.0007785	-0.0004369
29	0.0003674	-0.01432	0.2931	-0.03858	0.02029	-0.003276	0.0007164	-0.0004009
30	0.0003382	-0.01375	0.2927	-0.03707	0.01946	-0.003121	0.0006611	-0.0003689

Table A.3

Moments for the axial-vector correlator in the $\overline{\text{MS}}$ scheme

n	$C_n^{(0),a}$	$C_n^{(1),a}$	$C_{A,n}^{(2),a}$	$C_{NA,n}^{(2),a}$	$C_{l,n}^{(2),a}$	$C_{F,n}^{(2),a}$	$C_{S,n}^{(2),a}[1]$	$C_{S,n}^{(2),a}[L]$
1	0.5333	1.701	2.314	2.714	-1.046	0.3433	1.970	-0.6914
2	0.1524	0.7158	1.648	1.693	-0.6638	0.06509	0.3832	-0.1867
3	0.06772	0.3968	1.190	1.090	-0.4313	0.02238	0.1447	-0.08050
4	0.03694	0.2524	0.8998	0.7579	-0.3015	0.01013	0.07290	-0.04309
5	0.02273	0.1748	0.7077	0.5583	-0.2228	0.005396	0.04308	-0.02618
6	0.01516	0.1282	0.5741	0.4293	-0.1717	0.003202	0.02813	-0.01729
7	0.01070	0.09805	0.4772	0.3409	-0.1366	0.002052	0.01966	-0.01212
8	0.007883	0.07743	0.4045	0.2778	-0.1114	0.001393	0.01443	-0.008880
9	0.006006	0.06270	0.3484	0.2310	-0.09269	0.0009894	0.01098	-0.006736
10	0.004700	0.05181	0.3040	0.1954	-0.07843	0.0007283	0.008609	-0.005252
11	0.003760	0.04353	0.2683	0.1675	-0.06728	0.0005520	0.006905	-0.004189
12	0.003064	0.03709	0.2390	0.1454	-0.05840	0.0004287	0.005646	-0.003404
13	0.002536	0.03199	0.2147	0.1275	-0.05120	0.0003399	0.004690	-0.002811
14	0.002127	0.02787	0.1942	0.1127	-0.04529	0.0002742	0.003949	-0.002353
15	0.001804	0.02450	0.1768	0.1005	-0.04036	0.0002246	0.003364	-0.001993
16	0.001547	0.02170	0.1618	0.09013	-0.03621	0.0001864	0.002895	-0.001706
17	0.001338	0.01936	0.1488	0.08136	-0.03269	0.0001566	0.002514	-0.001473
18	0.001166	0.01738	0.1375	0.07384	-0.02967	0.0001329	0.002200	-0.001283
19	0.001024	0.01569	0.1275	0.06734	-0.02705	0.0001138	0.001938	-0.001125
20	0.0009049	0.01424	0.1187	0.06168	-0.02478	0.00009826	0.001719	-0.0009933
21	0.0008043	0.01297	0.1109	0.05672	-0.02278	0.00008549	0.001533	-0.0008821
22	0.0007188	0.01187	0.1038	0.05236	-0.02103	0.00007488	0.001375	-0.0007876
23	0.0006454	0.01091	0.09753	0.04849	-0.01947	0.00006599	0.001238	-0.0007067
24	0.0005821	0.01005	0.09183	0.04504	-0.01808	0.00005849	0.001120	-0.0006370
25	0.0005272	0.009298	0.08668	0.04196	-0.01684	0.00005211	0.001017	-0.0005765
26	0.0004793	0.008624	0.08198	0.03919	-0.01573	0.00004664	0.0009275	-0.0005238
27	0.0004372	0.008021	0.07770	0.03669	-0.01473	0.00004194	0.0008484	-0.0004776
28	0.0004002	0.007479	0.07377	0.03443	-0.01382	0.00003786	0.0007785	-0.0004369
29	0.0003674	0.006991	0.07017	0.03238	-0.01299	0.00003431	0.0007164	-0.0004009
30	0.0003382	0.006548	0.06685	0.03051	-0.01224	0.00003120	0.0006611	-0.0003689

Table A.4

Moments for the axial-vector correlator in the onshell scheme

n	$C_n^{(0),s}$	$C_n^{(1),s}$	$C_{A,n}^{(2),s}$	$C_{NA,n}^{(2),s}$	$C_{l,n}^{(2),s}$	$C_{F,n}^{(2),s}$	$C_{S,n}^{(2),s}[1]$	$C_{S,n}^{(2),s}[L]$
1	0.8000	0.4519	0.03484	-2.511	0.8815	0.7186	2.353	-0.4444
2	0.2286	0.3194	0.5536	-0.6269	0.3550	0.1201	0.8228	-0.2074
3	0.1016	0.1152	0.4516	-0.3544	0.2345	0.008315	0.3660	-0.1089
4	0.05541	0.02460	0.3448	-0.2797	0.1857	-0.01803	0.1923	-0.06377
5	0.03410	-0.01630	0.2876	-0.2439	0.1570	-0.02406	0.1134	-0.04057
6	0.02273	-0.03517	0.2635	-0.2193	0.1366	-0.02428	0.07267	-0.02746
7	0.01605	-0.04364	0.2577	-0.1995	0.1210	-0.02277	0.04956	-0.01950
8	0.01182	-0.04691	0.2614	-0.1827	0.1083	-0.02083	0.03546	-0.01438
9	0.009009	-0.04752	0.2698	-0.1681	0.09788	-0.01890	0.02635	-0.01093
10	0.007050	-0.04673	0.2803	-0.1553	0.08908	-0.01713	0.02019	-0.008525
11	0.005640	-0.04524	0.2913	-0.1440	0.08156	-0.01556	0.01586	-0.006789
12	0.004596	-0.04342	0.3021	-0.1339	0.07508	-0.01417	0.01273	-0.005505
13	0.003803	-0.04146	0.3124	-0.1250	0.06943	-0.01296	0.01040	-0.004532
14	0.003190	-0.03949	0.3219	-0.1170	0.06448	-0.01190	0.008624	-0.003782
15	0.002707	-0.03756	0.3305	-0.1098	0.06010	-0.01096	0.007246	-0.003193
16	0.002320	-0.03571	0.3383	-0.1033	0.05621	-0.01014	0.006159	-0.002723
17	0.002006	-0.03397	0.3454	-0.09739	0.05273	-0.009409	0.005287	-0.002344
18	0.001749	-0.03232	0.3516	-0.09205	0.04960	-0.008759	0.004580	-0.002034
19	0.001536	-0.03078	0.3572	-0.08719	0.04678	-0.008178	0.003998	-0.001778
20	0.001357	-0.02934	0.3622	-0.08274	0.04422	-0.007656	0.003516	-0.001565
21	0.001206	-0.02799	0.3665	-0.07866	0.04189	-0.007187	0.003111	-0.001385
22	0.001078	-0.02674	0.3704	-0.07491	0.03976	-0.006763	0.002769	-0.001233
23	0.0009681	-0.02556	0.3738	-0.07145	0.03781	-0.006378	0.002478	-0.001103
24	0.0008732	-0.02447	0.3767	-0.06826	0.03602	-0.006027	0.002228	-0.0009917
25	0.0007908	-0.02344	0.3793	-0.06530	0.03437	-0.005707	0.002012	-0.0008952
26	0.0007189	-0.02249	0.3816	-0.06255	0.03285	-0.005415	0.001825	-0.0008113
27	0.0006559	-0.02159	0.3835	-0.05999	0.03144	-0.005146	0.001661	-0.0007379
28	0.0006003	-0.02075	0.3852	-0.05761	0.03012	-0.004898	0.001517	-0.0006734
29	0.0005511	-0.01996	0.3866	-0.05538	0.02890	-0.004669	0.001390	-0.0006165
30	0.0005073	-0.01922	0.3878	-0.05329	0.02776	-0.004458	0.001278	-0.0005661

Table A.5

Moments for the scalar correlator in the $\overline{\text{MS}}$ scheme

n	$C_n^{(0),s}$	$C_n^{(1),s}$	$C_{A,n}^{(2),s}$	$C_{NA,n}^{(2),s}$	$C_{l,n}^{(2),s}$	$C_{Fn}^{(2),s}$	$C_{S,n}^{(2),s}[1]$	$C_{S,n}^{(2),s}[L]$
1	0.8000	0.4519	0.03484	-2.511	0.8815	0.7186	2.353	-0.4444
2	0.2286	0.7765	1.426	0.8955	-0.3591	0.1911	0.8228	-0.2074
3	0.1016	0.5215	1.526	0.9989	-0.4002	0.07144	0.3660	-0.1089
4	0.05541	0.3571	1.327	0.8275	-0.3336	0.03362	0.1923	-0.06377
5	0.03410	0.2565	1.115	0.6646	-0.2691	0.01832	0.1134	-0.04057
6	0.02273	0.1922	0.9371	0.5378	-0.2185	0.01103	0.07267	-0.02746
7	0.01605	0.1489	0.7952	0.4417	-0.1798	0.007146	0.04956	-0.01950
8	0.01182	0.1186	0.6824	0.3685	-0.1502	0.004890	0.03546	-0.01438
9	0.009009	0.09662	0.5921	0.3119	-0.1273	0.003494	0.02635	-0.01093
10	0.007050	0.08017	0.5191	0.2673	-0.1092	0.002584	0.02019	-0.008525
11	0.005640	0.06756	0.4592	0.2317	-0.09464	0.001967	0.01586	-0.006789
12	0.004596	0.05769	0.4096	0.2028	-0.08285	0.001532	0.01273	-0.005505
13	0.003803	0.04982	0.3681	0.1790	-0.07315	0.001218	0.01040	-0.004532
14	0.003190	0.04345	0.3329	0.1592	-0.06508	0.0009850	0.008624	-0.003782
15	0.002707	0.03823	0.3028	0.1426	-0.05828	0.0008084	0.007246	-0.003193
16	0.002320	0.03388	0.2769	0.1285	-0.05251	0.0006722	0.006159	-0.002723
17	0.002006	0.03024	0.2544	0.1164	-0.04757	0.0005654	0.005287	-0.002344
18	0.001749	0.02715	0.2347	0.1060	-0.04330	0.0004804	0.004580	-0.002034
19	0.001536	0.02451	0.2174	0.09695	-0.03959	0.0004119	0.003998	-0.001778
20	0.001357	0.02224	0.2020	0.08903	-0.03635	0.0003561	0.003516	-0.001565
21	0.001206	0.02027	0.1884	0.08206	-0.03349	0.0003101	0.003111	-0.001385
22	0.001078	0.01855	0.1762	0.07589	-0.03097	0.0002719	0.002769	-0.001233
23	0.0009681	0.01703	0.1653	0.07041	-0.02872	0.0002398	0.002478	-0.001103
24	0.0008732	0.01570	0.1554	0.06551	-0.02672	0.0002127	0.002228	-0.0009917
25	0.0007908	0.01451	0.1464	0.06112	-0.02492	0.0001896	0.002012	-0.0008952
26	0.0007189	0.01346	0.1383	0.05716	-0.02330	0.0001698	0.001825	-0.0008113
27	0.0006559	0.01252	0.1309	0.05359	-0.02184	0.0001528	0.001661	-0.0007379
28	0.0006003	0.01167	0.1241	0.05035	-0.02051	0.0001380	0.001517	-0.0006734
29	0.0005511	0.01090	0.1179	0.04739	-0.01930	0.0001251	0.001390	-0.0006165
30	0.0005073	0.01021	0.1122	0.04470	-0.01820	0.0001138	0.001278	-0.0005661

Table A.6

Moments for the scalar correlator in the onshell scheme

n	$C_n^{(0),p}$	$C_n^{(1),p}$	$C_{A,n}^{(2),p}$	$C_{NA,n}^{(2),p}$	$C_{l,n}^{(2),p}$	$C_{F,n}^{(2),p}$	$C_{S,n}^{(2),p}[1]$	$C_{S,n}^{(2),p}[L]$
1	1.333	2.333	2.712	-1.858	0.9259	1.311	5.629	-1.000
2	0.5333	1.548	3.399	0.02615	0.4346	0.3307	3.065	-0.6667
3	0.3048	0.9088	2.797	0.04435	0.4017	0.06951	1.952	-0.4667
4	0.2032	0.5346	2.198	-0.1204	0.4294	-0.02758	1.375	-0.3471
5	0.1478	0.3010	1.774	-0.2777	0.4600	-0.07127	1.034	-0.2703
6	0.1137	0.1458	1.506	-0.4046	0.4846	-0.09305	0.8132	-0.2180
7	0.09093	0.03751	1.358	-0.5039	0.5029	-0.1044	0.6612	-0.1804
8	0.07488	-0.04085	1.300	-0.5813	0.5162	-0.1104	0.5512	-0.1525
9	0.06306	-0.09923	1.310	-0.6422	0.5256	-0.1133	0.4686	-0.1311
10	0.05405	-0.1437	1.369	-0.6903	0.5320	-0.1144	0.4048	-0.1142
11	0.04700	-0.1783	1.467	-0.7286	0.5362	-0.1145	0.3542	-0.1007
12	0.04136	-0.2055	1.595	-0.7594	0.5386	-0.1139	0.3134	-0.08963
13	0.03677	-0.2271	1.745	-0.7842	0.5398	-0.1128	0.2798	-0.08044
14	0.03296	-0.2446	1.913	-0.8042	0.5400	-0.1116	0.2519	-0.07273
15	0.02977	-0.2587	2.095	-0.8205	0.5394	-0.1101	0.2283	-0.06617
16	0.02707	-0.2702	2.288	-0.8336	0.5383	-0.1086	0.2082	-0.06054
17	0.02475	-0.2796	2.490	-0.8442	0.5367	-0.1071	0.1908	-0.05566
18	0.02274	-0.2874	2.699	-0.8527	0.5347	-0.1056	0.1758	-0.05141
19	0.02099	-0.2937	2.913	-0.8595	0.5324	-0.1040	0.1626	-0.04767
20	0.01945	-0.2989	3.131	-0.8649	0.5299	-0.1025	0.1510	-0.04436
21	0.01810	-0.3032	3.353	-0.8690	0.5273	-0.1010	0.1407	-0.04142
22	0.01689	-0.3067	3.577	-0.8721	0.5246	-0.09956	0.1315	-0.03879
23	0.01581	-0.3095	3.803	-0.8744	0.5217	-0.09814	0.1233	-0.03642
24	0.01484	-0.3118	4.030	-0.8759	0.5188	-0.09677	0.1159	-0.03429
25	0.01397	-0.3136	4.258	-0.8768	0.5159	-0.09544	0.1092	-0.03236
26	0.01318	-0.3150	4.487	-0.8771	0.5129	-0.09415	0.1032	-0.03060
27	0.01246	-0.3160	4.715	-0.8770	0.5099	-0.09291	0.09765	-0.02899
28	0.01181	-0.3168	4.944	-0.8765	0.5069	-0.09170	0.09260	-0.02752
29	0.01121	-0.3173	5.173	-0.8757	0.5039	-0.09053	0.08797	-0.02618
30	0.01065	-0.3176	5.401	-0.8746	0.5009	-0.08940	0.08372	-0.02493

Table A.7

Moments for the pseudo-scalar correlator in the $\overline{\text{MS}}$ scheme

n	$C_n^{(0),p}$	$C_n^{(1),p}$	$C_{A,n}^{(2),p}$	$C_{NA,n}^{(2),p}$	$C_{l,n}^{(2),p}$	$C_{F,n}^{(2),p}$	$C_{S,n}^{(2),p}[1]$	$C_{S,n}^{(2),p}[L]$
1	1.333	2.333	2.712	-1.858	0.9259	1.311	5.629	-1.000
2	0.5333	2.615	7.040	3.578	-1.232	0.4964	3.065	-0.6667
3	0.3048	2.128	8.273	4.104	-1.502	0.2589	1.952	-0.4667
4	0.2032	1.754	8.466	3.939	-1.475	0.1618	1.375	-0.3471
5	0.1478	1.483	8.331	3.659	-1.387	0.1124	1.034	-0.2703
6	0.1137	1.282	8.090	3.381	-1.291	0.08353	0.8132	-0.2180
7	0.09093	1.129	7.821	3.130	-1.202	0.06509	0.6612	-0.1804
8	0.07488	1.008	7.554	2.910	-1.121	0.05249	0.5512	-0.1525
9	0.06306	0.9097	7.300	2.718	-1.050	0.04347	0.4686	-0.1311
10	0.05405	0.8292	7.062	2.550	-0.9878	0.03674	0.4048	-0.1142
11	0.04700	0.7618	6.842	2.402	-0.9322	0.03157	0.3542	-0.1007
12	0.04136	0.7045	6.639	2.271	-0.8828	0.02751	0.3134	-0.08963
13	0.03677	0.6553	6.451	2.154	-0.8385	0.02424	0.2798	-0.08044
14	0.03296	0.6125	6.276	2.050	-0.7987	0.02157	0.2519	-0.07273
15	0.02977	0.5749	6.115	1.956	-0.7627	0.01936	0.2283	-0.06617
16	0.02707	0.5418	5.965	1.871	-0.7301	0.01749	0.2082	-0.06054
17	0.02475	0.5122	5.825	1.793	-0.7003	0.01591	0.1908	-0.05566
18	0.02274	0.4858	5.694	1.722	-0.6730	0.01455	0.1758	-0.05141
19	0.02099	0.4619	5.571	1.657	-0.6480	0.01338	0.1626	-0.04767
20	0.01945	0.4403	5.456	1.597	-0.6248	0.01235	0.1510	-0.04436
21	0.01810	0.4207	5.348	1.542	-0.6034	0.01145	0.1407	-0.04142
22	0.01689	0.4027	5.246	1.490	-0.5836	0.01065	0.1315	-0.03879
23	0.01581	0.3862	5.150	1.443	-0.5651	0.009943	0.1233	-0.03642
24	0.01484	0.3710	5.059	1.398	-0.5478	0.009309	0.1159	-0.03429
25	0.01397	0.3570	4.972	1.357	-0.5317	0.008739	0.1092	-0.03236
26	0.01318	0.3440	4.890	1.318	-0.5166	0.008225	0.1032	-0.03060
27	0.01246	0.3320	4.812	1.281	-0.5023	0.007760	0.09765	-0.02899
28	0.01181	0.3207	4.737	1.247	-0.4889	0.007337	0.09260	-0.02752
29	0.01121	0.3102	4.666	1.214	-0.4763	0.006951	0.08797	-0.02618
30	0.01065	0.3004	4.598	1.183	-0.4643	0.006597	0.08372	-0.02493

Table A.8
Moments for the pseudo-scalar correlator in the onshell scheme

B Analytical Results

In this appendix we present the analytical results for the moments 9 to 12 of the various currents in the $\overline{\text{MS}}$ -scheme. The expression for the moments up to 30 can be obtained from

<http://www-ttp.particle.uni-karlsruhe.de/Progdata/ttp07/ttp07-32> in computer readable form in the $\overline{\text{MS}}$ and onshell scheme. In the following expressions we use $L = \log \mu^2/m^2$ and $L_{-q^2} = \log(-q^2/m^2)$. The singlet contributions $C_{S,n}^{(2),\delta}$ are always given separately.

B.1 Scalar Current

$$\sum_{n=9}^{12} C_n^{(0),s} z^n = \frac{131072}{14549535} z^9 + \frac{262144}{37182145} z^{10} + \frac{1048576}{185910725} z^{11} + \frac{2097152}{456326325} z^{12}$$

$$\begin{aligned} \sum_{n=9}^{12} C_n^{(1),s} z^n &= \left(-\frac{4979043746471936}{104786039514531375} - \frac{524288}{4849845} L \right) z^9 \\ &\quad + \left(-\frac{2888036521295872}{61796895098313375} - \frac{3538944}{37182145} L \right) z^{10} \\ &\quad + \left(-\frac{38132976301932544}{842822916656645925} - \frac{3145728}{37182145} L \right) z^{11} \\ &\quad + \left(-\frac{33183292389464276992}{764287144877276645625} - \frac{11534336}{152108775} L \right) z^{12} \end{aligned}$$

$$\begin{aligned} C_9^{(2),s} &= \left(\frac{1048576}{1616615} L^2 + \frac{25108082269650944}{34928679838177125} L \right. \\ &\quad \left. + \frac{73746539708944133873833421163704138849}{5771391802019474808577720320000} - \frac{3409922386710494034767011}{320780855251304448} \zeta_3 \right) C_F^2 \\ &\quad + C_A \left(-\frac{65536}{1322685} L^2 - \frac{5406868428560384}{28578010776690375} L \right. \\ &\quad \left. + \frac{102915497024490763942656449854922612500879}{437529212511096385238276977459200000} - \frac{1345087895588279678743561}{6873875469670809600} \zeta_3 \right) C_F \end{aligned}$$

$$\begin{aligned}
& + T_F \left(\left(\frac{262144}{14549535} n_h + \frac{262144}{14549535} n_l \right) L^2 + \left(\frac{14418875171495936}{314358118543594125} n_h \right. \right. \\
& + \frac{14418875171495936}{314358118543594125} n_l \Big) L - \frac{370939064258803430677307}{488861314420492468224000} n_h \\
& \left. \left. + \frac{12790934874367656891392}{130678984236690621356625} n_l + \frac{125624633262191}{204096845905920} n_h \zeta_3 \right) C_F \right)
\end{aligned}$$

$$\begin{aligned}
C_{10}^{(2),s} = & \left(\frac{23887872}{37182145} L^2 + \frac{1743551373172736}{2288773892530125} L \right. \\
& + \frac{1181283682867330857434847115794497652295927361}{18741992087247811295709473066188800000} \\
& \left. - \frac{1856910365195457777240839095367}{35414206419744011059200} \zeta_3 \right) C_F^2 \\
& + C_A \left(- \frac{147456}{3380195} L^2 - \frac{2883103404986368}{16853698663176375} L \right. \\
& + \frac{19485093544688649029885182650128118344232413}{20183683786266873703071740225126400000} \\
& \left. - \frac{738743868672823822714945309}{919849517395948339200} \zeta_3 \right) C_F \\
& + T_F \left(\left(\frac{589824}{37182145} n_h + \frac{589824}{37182145} n_l \right) L^2 + \left(\frac{7789487453519872}{185390685294940125} n_h \right. \right. \\
& + \frac{7789487453519872}{185390685294940125} n_l \Big) L - \frac{4979656088382493508774203867}{6626352163198301909286912000} n_h \\
& \left. \left. + \frac{48054627678191205275648}{539469652874543334318375} n_l + \frac{332499096340061}{544258255749120} n_h \zeta_3 \right) C_F \right)
\end{aligned}$$

$$\begin{aligned}
C_{11}^{(2),s} = & \left(\frac{4718592}{7436429} L^2 + \frac{8933862862782464}{11237638888755279} L \right. \\
& + \frac{7404906335674218474752347314237559396292812077443}{24289621745073163439239477093780684800000} \\
& \left. - \frac{61139862184252373166516579786803}{241074161519130140737536} \zeta_3 \right) C_F^2 + C_A \left(- \frac{131072}{3380195} L^2 \right.
\end{aligned}$$

$$\begin{aligned}
& - \frac{1880663970832384}{12097936602726975} L \\
& + \frac{8830293913654550377524203305197260449225292386979}{2237852825236511033113012799650733752320000} \\
& - \frac{209352182103823255038597110761}{63776233206119084851200} \zeta_3 C_F + T_F \left(\left(\frac{524288}{37182145} n_h + \frac{524288}{37182145} n_l \right) L^2 \right. \\
& \left. + \left(\frac{97554230956294144}{2528468749969937775} n_h + \frac{97554230956294144}{2528468749969937775} n_l \right) L \right. \\
& \left. - \frac{202040916959120787173924674741}{271479640140730429738057728000} n_h + \frac{394357158107030025924608}{4835000144023764273824265} n_l \right. \\
& \left. + \frac{2287436936895761}{3773523906527232} n_h \zeta_3 \right) C_F
\end{aligned}$$

$$\begin{aligned}
C_{12}^{(2),s} = & \left(\frac{31719424}{50702925} L^2 + \frac{19006459960269111296}{23160216511432625625} L \right. \\
& + \frac{188473078860503880648883122776543550015991250654673059}{129919789020675223866838798646389820620800000} \\
& - \frac{23090275323409880205366729096347}{19132869961835725455360} \zeta_3 \Big) C_F^2 + C_A \left(- \frac{15859712}{456326325} L^2 \right. \\
& \left. - \frac{29590089938919374848}{208441948602893630625} L \right. \\
& \left. + \frac{2086533237898744255234695965842642441637712801424593}{1299197890206752238668387986463898206208000000} \right. \\
& \left. - \frac{41752924406364782322130747883}{3121913513586248908800} \zeta_3 \right) C_F + T_F \left(\left(\frac{5767168}{456326325} n_h + \frac{5767168}{456326325} n_l \right) L^2 \right. \\
& \left. + \left(\frac{81479567700203732992}{2292861434631829936875} n_h + \frac{81479567700203732992}{2292861434631829936875} n_l \right) L \right. \\
& \left. - \frac{88884847785166765220997026873}{120599609370209094749021798400} n_h + \frac{41147533572114438909275987968}{548058254961784643538602765625} n_l \right. \\
& \left. + \frac{77358608492779}{128642860449792} n_h \zeta_3 \right) C_F
\end{aligned}$$

$$C_{S,9}^{(2),s} = - \frac{28771023505735526373476647}{1454362410400965092966400000} + \frac{143600001918689}{3741775508275200} \zeta_3 - \frac{289369094656}{26467422856875} L_{-q^2}$$

$$C_{S,10}^{(2),s} = -\frac{1090589835840240580931001947}{57980581427985141706260480000} + \frac{48559274491381}{1496710203310080}\zeta_3 - \frac{3471392768}{407191120875}L_{-q^2}$$

$$\begin{aligned} C_{S,11}^{(2),s} = & -\frac{115469790307862708811970912146409}{6584738671613416573296590192640000} + \frac{4337059242964423}{156086670679080960}\zeta_3 \\ & - \frac{225667578742784}{33237789623663625}L_{-q^2} \end{aligned}$$

$$\begin{aligned} C_{S,12}^{(2),s} = & -\frac{6397059251470658815951587545516867}{395084320296804994397795411558400000} + \frac{675994471643152871}{28095600722234572800}\zeta_3 \\ & - \frac{2744536517378048}{498566844354954375}L_{-q^2} \end{aligned}$$

B.2 Pseudo-Scalar Current

$$\sum_{n=9}^{12} C_n^{(0),p} z^n = +\frac{131072}{2078505}z^9 + \frac{262144}{4849845}z^{10} + \frac{1048576}{22309287}z^{11} + \frac{2097152}{50702925}z^{12}$$

$$\begin{aligned} \sum_{n=9}^{12} C_n^{(1),p} z^n = & \left(-\frac{49751393148928}{501368610117375} - \frac{524288}{692835}L \right) z^9 \\ & + \left(-\frac{557796221206528}{3880964426464125} - \frac{1179648}{1616615}L \right) z^{10} \\ & + \left(-\frac{4091600265773056}{22953132465087825} - \frac{5242880}{7436429}L \right) z^{11} \\ & + \left(-\frac{35891639960928256}{174694204543377519} - \frac{11534336}{16900975}L \right) z^{12} \end{aligned}$$

$$\begin{aligned} C_9^{(2),p} = & + C_F T_R \left(\frac{24213861812657343488}{46071664047183800025} n_l - \frac{23936615221766899739377}{13951233275688124416000} n_h \right. \\ & \left. + \frac{386477922523}{289910292480} n_h \zeta_3 + \frac{365917995900928}{1504105830352125} L(n_l + n_h) + \frac{262144}{2078505} L^2(n_l + n_h) \right) \end{aligned}$$

$$\begin{aligned}
& + C_F C_A \left(-\frac{2774476486497511252284870305976724044391}{9695938227392717678410570137600000} \right. \\
& + \frac{1870074094390219597606687}{7855857679623782400} \zeta_3 - \frac{151838577682432}{136736893668375} L - \frac{65536}{188955} L^2 \Big) \\
& + C_F^2 \left(-\frac{18248707238521284112217374676684189}{1201215870545458762874880000} \right. \\
& \left. + \frac{143085894538571009718455041}{11321677244163686400} \zeta_3 + \frac{372897204109312}{167122870039125} L + \frac{1048576}{230945} L^2 \right)
\end{aligned}$$

$$\begin{aligned}
C_{10}^{(2),p} = & + C_F T_R \left(\frac{18023374701238546946048}{33879736653956827759125} n_l - \frac{1835086571234207640548161}{941510679624652161024000} n_h \right. \\
& + \frac{46149597022417}{30236569763840} n_h \zeta_3 + \frac{2917754077462528}{11642893279392375} L(n_l + n_h) + \frac{196608}{1616615} L^2(n_l + n_h) \Big) \\
& + C_F C_A \left(-\frac{1539378756641920703135316484755839467328419}{1333422361938579459773796502732800000} \right. \\
& + \frac{12803248135021178751056537}{13331152426028236800} \zeta_3 - \frac{1179975928287232}{1058444843581125} L - \frac{49152}{146965} L^2 \Big) \\
& + C_F^2 \left(-\frac{27324314428644557274188086091814971713169}{369369075329246387748974100480000} \right. \\
& \left. + \frac{13536779710726154580166718023}{219964015029465907200} \zeta_3 + \frac{423117757374464}{143739423202375} L + \frac{7962624}{1616615} L^2 \right)
\end{aligned}$$

$$\begin{aligned}
C_{11}^{(2),p} = & C_F T_R \left(\frac{3760136484063862872174592}{7013105487369063346138875} n_l - \frac{14436891835130136916846548977}{6626352163198301909286912000} n_h \right. \\
& + \frac{186926938565003}{108851651149824} n_h \zeta_3 + \frac{17577073730093056}{68859397395263475} L(n_l + n_h) + \frac{2621440}{22309287} L^2(n_l + n_h) \Big) \\
& + C_F C_A \left(-\frac{2196670741691390865449882336983942060570342639}{472298200598644844651878721267957760000} \right. \\
& + \frac{5140924281484864972357892859}{1328671525127480934400} \zeta_3 - \frac{6968767912075264}{6259945217751225} L - \frac{655360}{2028117} L^2 \Big) \\
& + C_F^2 \left(-\frac{19892582218578011106338578696247144162810751553}{56225976261743433887128419198566400000} \right)
\end{aligned}$$

$$+ \frac{821232360279025582272054039829}{2790210202767709962240} \zeta_3 + \frac{796428906692608}{218601261572265} L + \frac{39321600}{7436429} L^2 \Big)$$

$$\begin{aligned} C_{12}^{(2),p} = & C_F T_R \left(\frac{2361650790215100407548239872}{4384466039694277148308822125} n_l - \frac{43084675796375645372731027301693}{17917656249288208362711810048000} n_h \right. \\ & + \frac{3922441614750337}{2058285767196672} n_h \zeta_3 + \frac{676219888715104256}{2620413068150662785} L(n_l + n_h) + \frac{5767168}{50702925} L^2(n_l + n_h) \Big) \\ & + C_F C_A \left(- \frac{70034794682581481813249178402809862391078239422033231}{3741689923795446447364957401016026833879040000} \right. \\ & + \frac{77778913328384051652725192513}{4995061621737998254080} \zeta_3 - \frac{1319456473035685888}{1191096849159392175} L - \frac{15859712}{50702925} L^2 \Big) \\ & + C_F^2 \left(- \frac{2267473277094876433590459813785417415724639080638329}{1360218817724097152597410717251718348800000} \right. \\ & \left. + \frac{66863488712130988880884620697226071}{48214832303826028147507200} \zeta_3 + \frac{572835921739218944}{132344094351043575} L + \frac{95158272}{16900975} L^2 \right) \end{aligned}$$

$$\begin{aligned} C_{S,9}^{(2),p} = & + \frac{27352144660490483390633}{174887254737970790400000} + \frac{2454162037509}{9448928051200} \zeta_3 - \frac{263495168}{2010133125} L_{-q^2} \\ C_{S,10}^{(2),p} = & + \frac{99214339418590131445021}{783494901226109140992000} + \frac{46177240370863}{199561360441344} \zeta_3 - \frac{732934144}{6416344935} L_{-q^2} \\ C_{S,11}^{(2),p} = & + \frac{2787996822340736999889074473}{26799913193379798833115955200} + \frac{53552348130925}{257285720899584} \zeta_3 - \frac{21320382464}{211739382855} L_{-q^2} \\ C_{S,12}^{(2),p} = & + \frac{14641282147919288479322671871}{169262609642398729472311296000} + \frac{561179696637195}{2973079441506304} \zeta_3 - \frac{1212441755648}{13527793904625} L_{-q^2} \end{aligned}$$

B.3 Vector Current

$$\sum_{n=9}^{12} C_n^{(0),v} z^n = \frac{524288}{8729721} z^9 + \frac{524288}{10140585} z^{10} + \frac{8388608}{185910725} z^{11} + \frac{4194304}{105306075} z^{12}$$

$$\begin{aligned}
\sum_{n=9}^{12} C_n^{(1),a} z^n = & \left(-\frac{2103270735183872}{8981660529816975} - \frac{262144}{323323} L \right) z^9 \\
& + \left(-\frac{57014372204019712}{219098082621292875} - \frac{524288}{676039} L \right) z^{10} \\
& + \left(-\frac{13456105329705877504}{48040906249428817725} - \frac{12582912}{16900975} L \right) z^{11} \\
& + \left(-\frac{249307596877594624}{843894528756654375} - \frac{8388608}{11700675} L \right) z^{12}
\end{aligned}$$

$$\begin{aligned}
C_9^{(2),v} = & \left(\frac{1769472}{323323} L^2 + \frac{1422485887860736}{332654093696925} L \right. \\
& - \frac{381427200524285859827479342961645120691697}{26317546617208805127114404659200000} \\
& + \left. \frac{4641207108486463789099278533}{384937026301565337600} \zeta_3 \right) C_F^2 + C_A \left(-\frac{32768}{88179} L^2 - \frac{3201458214330368}{2449543780859175} L \right. \\
& - \frac{4800616671655745922224061798696958246114657}{21001402200532626491437294918041600000} + \frac{62742999460179248975566471}{329946022544198860800} \zeta_3 \Big) C_F \\
& + T_R \left(\left(\frac{131072}{969969} n_h + \frac{131072}{969969} n_l \right) L^2 + \left(\frac{8171733794127872}{26944981589450925} n_h \right. \right. \\
& + \frac{8171733794127872}{26944981589450925} n_l \Big) L - \frac{7505222973653044996167293}{2893884388042736664576000} n_h \\
& \left. \left. + \frac{1716980884029425246777344}{2744258668970503048489125} n_l + \frac{15641077379375}{7653631721472} n_h \zeta_3 \right) C_F
\right)
\end{aligned}$$

$$\begin{aligned}
C_{10}^{(2),v} = & \left(\frac{3932160}{676039} L^2 + \frac{72590094055309312}{14606538841419525} L \right. \\
& - \frac{541634465543720570056096925789635688755714501}{7906777911807670390377433949798400000} \\
& + \left. \frac{3503779464918218459698976337}{61482997256500019200} \zeta_3 \right) C_F^2 \\
& + C_A \left(-\frac{720896}{2028117} L^2 - \frac{76685205430140928}{59754022533079875} L \right)
\end{aligned}$$

$$\begin{aligned}
& - \frac{100571880864387246559861014880105540717546397}{110694890765307385465284075297177600000} \\
& + \frac{358487787916859833012705187}{474297407407285862400} \zeta_3 \Big) C_F \\
& + T_R \left(\left(\frac{262144}{2028117} n_h + \frac{262144}{2028117} n_l \right) L^2 + \left(\frac{198611843579379712}{657294247863878625} n_h \right. \right. \\
& \left. \left. + \frac{198611843579379712}{657294247863878625} n_l \right) L - \frac{56043284857896604271843338613}{19879056489594905727860736000} n_h \right. \\
& \left. + \frac{1187963065976173458415616}{1912665132918835458037875} n_l + \frac{331575524130137}{148434069749760} n_h \zeta_3 \right) C_F
\end{aligned}$$

$$\begin{aligned}
C_{11}^{(2),v} = & \left(\frac{103809024}{16900975} L^2 + \frac{1643667546316865536}{291157007572295865} L \right. \\
& - \frac{1070887924864138198352946851863557684684339508412651}{3351967800820096554615047838941734502400000} \\
& \left. + \frac{9610834140751883729239482548466517}{36161124227869521110630400} \zeta_3 \right) C_F^2 \\
& + C_A \left(- \frac{5767168}{16900975} L^2 - \frac{16505631011785080832}{13102065340753313925} L \right. \\
& - \frac{10142587654701589960628097458296025022529793100251069}{2806267442846584835523718050762020125409280000} \\
& \left. + \frac{1150547909207069411531224161671}{382657399236714509107200} \zeta_3 \right) C_F + T_R \left(\left(\frac{2097152}{16900975} n_h + \frac{2097152}{16900975} n_l \right) L^2 \right. \\
& + \left(\frac{43261806664333656064}{144122718748286453175} n_h + \frac{43261806664333656064}{144122718748286453175} n_l \right) L \\
& - \frac{85142270271685420818460662817}{27996337889512825566737203200} n_h + \frac{849053414353143539189776384}{1377975041046772818039915525} n_l \\
& \left. + \frac{428230928483939}{176883933118464} n_h \zeta_3 \right) C_F
\end{aligned}$$

$$C_{12}^{(2),v} = \left(\frac{8388608}{1300075} L^2 + \frac{591048256550862848}{93766058750739375} L \right)$$

$$\begin{aligned}
& - \frac{2120116328634260041790541524636709954701152751347827221}{1439111509152094787448060538852318013030400000} \\
& + \frac{16883124936978831575637459733931549}{13775666372521722327859200} \zeta_3 \Big) C_F^2 + C_A \left(- \frac{11534336}{35102025} L^2 \right. \\
& - \frac{284624595694944256}{230153053297269375} L - \frac{20238608949682386388157368187133321175530208319894383}{1406650347291521220813893759780461215744000000} \\
& + \frac{103631644405192190650944065895}{8658106811012530307072} \zeta_3 \Big) C_F + T_R \left(\left(\frac{4194304}{35102025} n_h + \frac{4194304}{35102025} n_l \right) L^2 \right. \\
& + \left(\frac{753487939399450624}{2531683586269963125} n_h + \frac{753487939399450624}{2531683586269963125} n_l \right) L \\
& - \frac{213296190145039197864108250117409}{65438396736530847933382262784000} n_h + \frac{369724970712395017121284096}{605143454135205716089734375} n_l \\
& \left. + \frac{4949453959637945}{1899956092796928} n_h \zeta_3 \right) C_F
\end{aligned}$$

B.4 Axial-Vector Current

$$\sum_{n=9}^{12} C_n^{(0),a} z^n = \frac{262144}{43648605} z^9 + \frac{524288}{111546435} z^{10} + \frac{2097152}{557732175} z^{11} + \frac{4194304}{1368978975} z^{12}$$

$$\begin{aligned}
\sum_{n=9}^{12} C_n^{(1),a} z^n &= \left(- \frac{14273234676170752}{314358118543594125} - \frac{131072}{1616615} L \right) z^9 \\
&+ \left(- \frac{101689470330109952}{2410078908834221625} - \frac{524288}{7436429} L \right) z^{10} \\
&+ \left(- \frac{14155800052957184}{361209821424276825} - \frac{1048576}{16900975} L \right) z^{11} \\
&+ \left(- \frac{83544812412930228224}{2292861434631829936875} - \frac{8388608}{152108775} L \right) z^{12}
\end{aligned}$$

$$C_9^{(2),a} = C_F T_R \left(\frac{209029528206436443461632}{2744258668970503048489125} n_l - \frac{721707504396631265775619523}{1296460205843146025730048000} n_h \right)$$

$$\begin{aligned}
& + \frac{1102011173546563}{2449162150871040} n_h \zeta_3 + \frac{35512855382474752}{943074355630782375} L(n_l + n_h) + \frac{65536}{4849845} L^2(n_l + n_h) \Big) \\
& + C_F C_A \left(\frac{2044821895603527816981536356704130687706357}{3360224352085220238629967186886656000} \right. \\
& - \frac{668136450989003773285863131}{1319784090176795443200} \zeta_3 - \frac{12933050525913088}{85734032330071125} L - \frac{16384}{440895} L^2 \Big) \\
& + C_F^2 \left(\frac{217311353924672252345666774738607455908207}{5540536129938695816234611507200000} \right. \\
& - \frac{4567332086889583465526764451}{139977100473296486400} \zeta_3 + \frac{8434594159026176}{11642893279392375} L + \frac{884736}{1616615} L^2 \Big)
\end{aligned}$$

$$\begin{aligned}
C_{10}^{(2),a} = & C_F T_R \left(\frac{287854153300932624846848}{4207863292421438007683325} n_l - \frac{209290713314001851931555887}{382289547876825110151168000} n_h \right. \\
& + \frac{181196559131413}{408193691811840} n_h \zeta_3 + \frac{243286941705469952}{7230236726502664875} L(n_l + n_h) + \frac{262144}{22309287} L^2(n_l + n_h) \Big) \\
& + C_F C_A \left(\frac{8649742991474532665515591016625431163403791601}{3542236504489836334889090409509683200000} \right. \\
& - \frac{44535077782003477491448862123}{21923080164603435417600} \zeta_3 - \frac{87853979961663488}{657294247863878625} L - \frac{65536}{2028117} L^2 \Big) \\
& + C_F^2 \left(\frac{3633687108507123867092545337354886401661662813}{19462837936757342499390606645657600000} \right. \\
& - \frac{35752565032549034445184262371577}{230192341728336071884800} \zeta_3 + \frac{117265192181399552}{160671927255614775} L + \frac{3932160}{7436429} L^2 \Big)
\end{aligned}$$

$$\begin{aligned}
C_{11}^{(2),a} = & C_F T_R \left(\frac{157211774390308655582420992}{2538375075612476243757739125} n_l - \frac{175561738935918272688195117821}{325775568168876515685669273600} n_h \right. \\
& + \frac{9918778191302813}{22641143439163392} n_h \zeta_3 + \frac{32831051515756544}{1083629464272830475} L(n_l + n_h) + \frac{524288}{50702925} L^2(n_l + n_h) \Big) \\
& + C_F C_A \left(\frac{1157200807257694296198427317159640234150785132824303}{118158629172487782548367075821558742122496000} \right. \\
& - \frac{261883214808207508025819129858143}{32143221535884018765004800} \zeta_3 - \frac{619633587273728}{5184829972597275} L - \frac{1441792}{50702925} L^2 \Big)
\end{aligned}$$

$$\begin{aligned}
& + C_F^2 \left(\frac{325018733172338765882468493323383479610810052389621}{370968768470208314344748377432286822400000} \right. \\
& - \left. \frac{105426049549787146186606803725022377}{144644496911478084442521600} \zeta_3 + \frac{1602332519923712}{2189150432874405} L + \frac{8650752}{16900975} L^2 \right)
\end{aligned}$$

$$\begin{aligned}
C_{12}^{(2),a} = & C_F T_R \left(\frac{92827398267438355820629508096}{1644174764885353930615808296875} n_l - \frac{104450315270262159531899064503}{196742892149046993786639482880} n_h \right. \\
& + \frac{5341389426809173}{12349714603180032} n_h \zeta_3 + \frac{188918503999998132224}{6878584303895489810625} L(n_l + n_h) \\
& \left. + \frac{4194304}{456326325} L^2(n_l + n_h) \right) \\
& + C_F C_A \left(\frac{14691137807907519650408236687148333789997689179014563981}{374168992379544644736495740101602683387904000000} \right. \\
& - \frac{818111578538634207243886625532379}{25046666131857676959744000} \zeta_3 - \frac{67346421666621587456}{625325845808680891875} L - \frac{11534336}{456326325} L^2 \\
& \left. + C_F^2 \left(\frac{151997936918859535196394940736545376607752983761243261719}{374168992379544644736495740101602683387904000000} \right. \right. \\
& - \frac{3258783646497863020834421263009179937}{964296646076520562950144000} \zeta_3 \\
& \left. \left. + \frac{186408134950156238848}{254762381625758881875} L + \frac{8388608}{16900975} L^2 \right) \right)
\end{aligned}$$

$$\begin{aligned}
C_{S,9}^{(2),a} = & - \frac{54729591036013756991855587205067403}{2933529196264874811502352306012160000} + \frac{24604386555649}{997806802206720} \zeta_3 \\
& - \frac{6722140930048}{997962281090775} L_{-q^2}
\end{aligned}$$

$$\begin{aligned}
C_{S,10}^{(2),a} = & - \frac{119621269712255836267447988400312983}{7360491437900958617951356695085056000} + \frac{87798501391061}{4245214394843136} \zeta_3 \\
& - \frac{303225290752}{57733355104425} L_{-q^2}
\end{aligned}$$

$$\begin{aligned}
C_{S,11}^{(2),a} = & - \frac{392233656487033430717559964717352391313}{27547265098473410838449785029714247680000} + \frac{2353323008444009}{133788574867783680} \zeta_3 \\
& - \frac{1219596674400256}{291157007572295865} L_{-q^2}
\end{aligned}$$

$$C_{S,12}^{(2),a} = -\frac{5473635073785826339847768690355966987576523}{436094396712755996196381981470399397888000000} + \frac{26173581704692859}{1728960044445204480}\zeta_3 \\ - \frac{466514873679872}{137042701251080625} L_{-q^2}$$

References

- [1] Shifman, M. A. and Vainshtein, A. I. and Zakharov, V. I. QCD and Resonance Physics: Applications. *Nucl. Phys.*, B147:448–518, 1979.
- [2] Reinders, L. J. and Rubinstein, H. and Yazaki, S. Hadron Properties from QCD Sum Rules. *Phys. Rept.*, 127:1, 1985.
- [3] Kuhn, J. H. and Steinhauser, M. and Sturm, C. Heavy quark masses from sum rules in four-loop approximation. *Nucl. Phys.*, B778:192–215, 2007.
- [4] Kuhn, J. H. and Steinhauser, M. Determination of α_s and heavy quark masses from recent measurements of R(s). *Nucl. Phys.*, B619:588–602, 2001.
- [5] Chetyrkin, K. G. and Kuhn, J. H. and Steinhauser, M. Heavy quark current correlators to $\mathcal{O}(\alpha_s^2)$. *Nucl. Phys.*, B505:40–64, 1997.
- [6] Broadhurst, D. J. Three loop on-shell charge renormalization without integration: Lambda-MS (QED) to four loops. *Z. Phys.*, C54:599–606, 1992.
- [7] Chetyrkin, K. G. and Kuhn, J. H. and Sturm, C. Four-loop moments of the heavy quark vacuum polarization function in perturbative QCD. *Eur. Phys. J.*, C48:107–110, 2006.
- [8] Boughezal, R. and Czakon, M. and Schutzmeier, T. Charm and bottom quark masses from perturbative QCD. *Phys. Rev.*, D74:074006, 2006.
- [9] Laporta, S. High-precision calculation of multi-loop Feynman integrals by difference equations. *Int. J. Mod. Phys.*, A15:5087–5159, 2000.
- [10] Chetyrkin, K. G. and Harlander, R. and Steinhauser, M. Singlet polarization functions at $\mathcal{O}(\alpha_s^2)$. *Phys. Rev.*, D58:014012, 1998.
- [11] Caffo, M. and Czyz, H. and Laporta, S. and Remiddi, E. The master differential equations for the 2-loop sunrise selfmass amplitudes. *Nuovo Cim.*, A111:365–389, 1998.
- [12] Remiddi, E. Differential equations for Feynman graph amplitudes. *Nuovo Cim.*, A110:1435–1452, 1997.
- [13] Boughezal, R. and Czakon, M. and Schutzmeier, T. Four-loop tadpoles: Applications in QCD. *Nucl. Phys. Proc. Suppl.*, 160:160–164, 2006.
- [14] Lepage, P. Private communication.

- [15] Nogueira, P. Automatic Feynman graph generation. *J. Comput. Phys.*, 105:279–289, 1993.
- [16] Seidensticker, T. Automatic application of successive asymptotic expansions of Feynman diagrams. *PhD thesis*, 1999.
- [17] Harlander, R. and Seidensticker, T. and Steinhauser, M. Complete corrections of $\mathcal{O}(\alpha\alpha_s)$ to the decay of the Z boson into bottom quarks. *Phys. Lett.*, B426:125–132, 1998.
- [18] Vermaseren, J. A. M. New features of FORM. *math-ph/0010025*, 2000.
- [19] Chetyrkin, K. G. and Tkachov, F. V. Integration by Parts: The Algorithm to Calculate beta Functions in 4 Loops. *Nucl. Phys.*, B192:159–204, 1981.
- [20] Laporta, S. and Remiddi, E. The analytical value of the electron (g-2) at order α^3 in QED. *Phys. Lett.*, B379:283–291, 1996.
- [21] Marquard, P. and Seidel, D. Crusher, an automated integral reduction setup. unpublished.
- [22] Bauer, C. and Frink, A. and Kreckel, R. Introduction to the GiNaC framework for symbolic computation within the C++ Programming Language. *Journal of Symbolic Computation*, 33:1, 2002.
- [23] Lewis, R. H. *Fermat's User Guide*.
- [24] Tentyukov, M. and Vermaseren, J. A. M. Extension of the functionality of the symbolic program FORM by external software. *Computer Physics Communications*, 176:385, 2007.
- [25] Tarasov, O. V. and Vladimirov, A. A. and Zharkov, A. Yu. The Gell-Mann-Low Function of QCD in the Three Loop Approximation. *Phys. Lett.*, B93:429–432, 1980.
- [26] Gray, N. and Broadhurst, D. J. and Grafe, W. and Schilcher, K. Three loop relation of quark (modified) MS and pole masses. *Z. Phys.*, C48:673–680, 1990.
- [27] Tarasov, O. V. Anomalous dimensions of quark masses in three loop approximation. *JINR-P2-82-900*.
- [28] Gorishnii, S. G. and Kataev, A. L. and Larin, S. A. Next next-to-leading perturbative QCD corrections and light quark masses. *Phys. Lett.*, B135:457, 1984.
- [29] Larin, S. A. The Renormalization of the axial anomaly in dimensional regularization. *Phys. Lett.*, B303:113–118, 1993.
- [30] Chetyrkin, K. G. and Kuhn, J. H. and Steinhauser, M. Higher moments of heavy quark vacuum polarization. *hep-ph/9607422*, 1996.
- [31] Czarnecki, A. and Melnikov, K. Two-loop QCD corrections to the heavy quark pair production cross section in $e^+ e^-$ annihilation near the threshold. *Phys. Rev. lett.*, 80:2531–2534, 1998.

- [32] Chetyrkin, K. G. and Kuhn, J. H. and Steinhauser, M. Three-loop polarization function and $\mathcal{O}(\alpha_s^2)$ corrections to the production of heavy quarks. *Nucl. Phys.*, B482:213–240, 1996.